Electronic Supplementary Information (ESI)

pH-Dependent Phosphate Separation using Tripodal Hexaurea Receptor

Zhong-Yu Sun, Si-Qi Chen, Lin Liang, Wei Zhao, Xiao-Juan Yang and Biao Wu**

Key Laboratory of Medicinal Molecule Science and Pharmaceutics Engineering, Ministry of Industry and Information Technology, School of Chemistry and Chemical Engineering, Beijing Institute of Technology, Beijing 102488, China.

Email: zhaochem@bit.edu.cn; wubiao@bit.edu.cn

Table of contents

S1. General Information

All starting materials and solvents were obtained from commercial sources (Beijing InnoChem, Aladdin, Macklin Science & Technology Co., Ltd.), which were used without further purification. ^{1}H and ^{31}P NMR spectra were recorded on Bruker AVANCE AV II-400/700 MHz spectrometer at 298 K. ^{1}H NMR chemical shifts were reported relative to residual solvent peaks (^{1}H NMR: 2.50 ppm for DMSO-d6, 7.26 ppm for $CDCl_3$;^{31}P NMR for -144 ppm for PF_6^-). Single crystal X-ray data were recorded on Bruker D8 Venture Photon II diffractometer. The anion concentration in aqueous solution was recorded by Shine ion chromatography (CIC-D100, China). All aqueous solutions were prepared by using ultrapure water (18.25 MΩ·cm).

The phosphate salts are not commercially available and were prepared by acid-base reaction from corresponding tetraalkylammonium hydroxide solution (water) and phosphoric acid. The phosphoric acid (H_3PO_4) was placed in a small vial and certain amounts of hydroxide was added. The mixture was diluted to 1 mL and the prepared solution was used directly or diluted to a certain concentration for titration.

TMA_3PO_4 (water): H_3PO_4 was mixed with three equivalents of TMAOH (40% wt, H_2O).

TBA_3PO_4 (water): $TBAH_2PO4$ was mixed with two equivalents of TBAOH (40% wt, H_2O).

TBA_2HPO_4 (water): $TBAH_2PO4$ was mixed with one equivalent of TBAOH (40% wt, H_2O).

S2. Synthetic Procedures of Hexaurea Receptor L

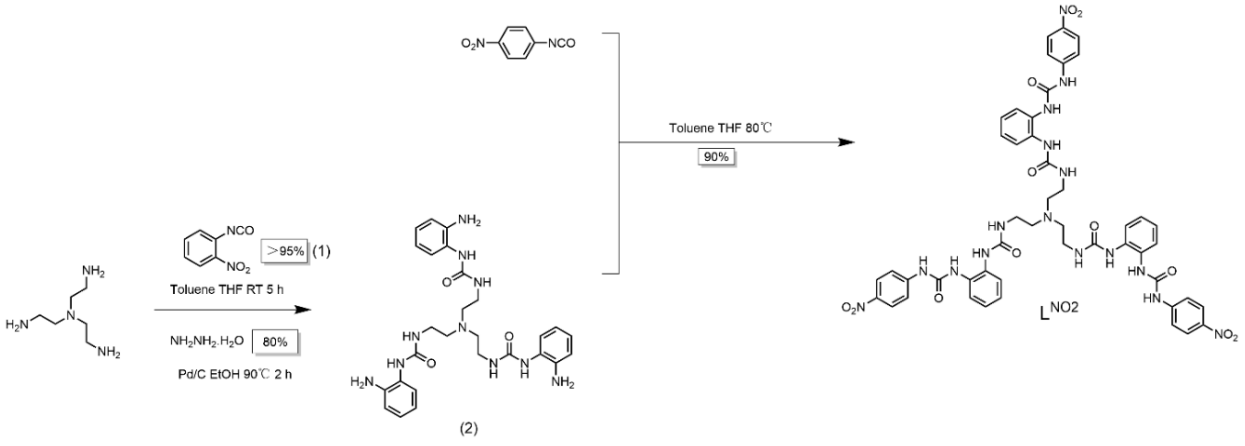

Figure S1. Synthetic scheme of preparing tripodal hexaurea receptor **L** according to previously reported procedures (*Angew. Chem., Int. Ed.* 2011, **50**, 486-490).

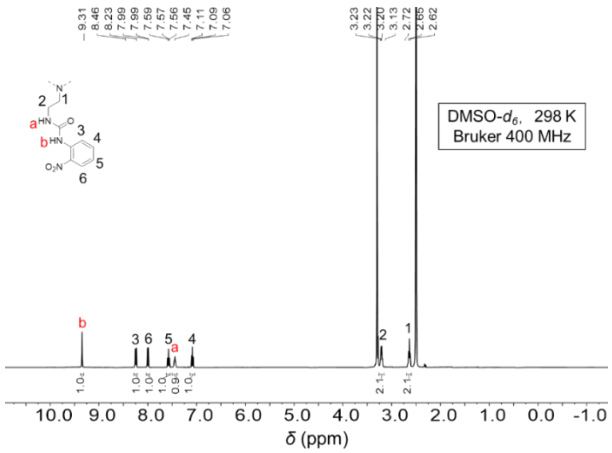

Figure S2 ^{1}H NMR spectrum (400 MHz, 298 K, DMSO-d_6) of compound 1.

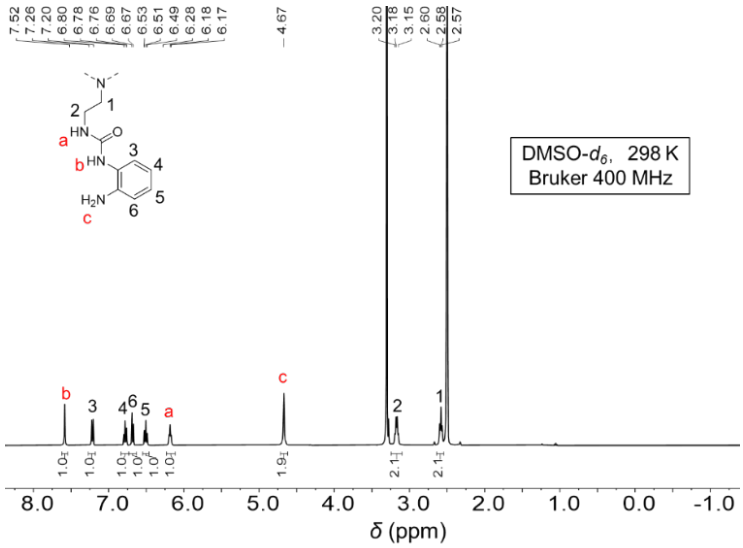

Figure S3 ^{1}H NMR spectrum (400 MHz, 298 K, DMSO-d_6) of compound 2

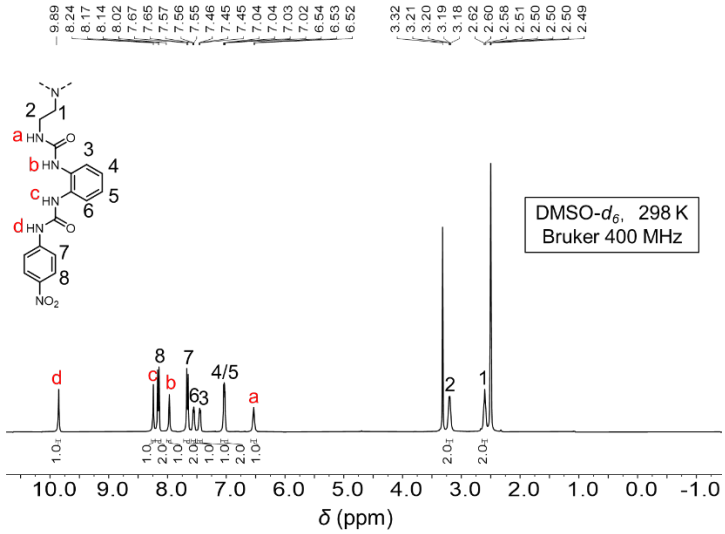

Figure S4 ^{1}H NMR spectrum (400 MHz, 298 K, DMSO-d_6) of receptor L^{NO2}

S3. Single Crystal X-ray Diffraction Structures

Table S1 Crystal data details for obtained phosphate binding complex.

Complex	PO_4^{3-} binding complex
CCDC	2290471
Empirical formula	$C_{64}H_{90}N_{21}O_{16}P$
Formula weight	1440.53
Crystal system	Orthorhombic
Space group	$P2_12_12$
a (Å)	21.9758(14)
b (Å)	23.4980(15)
c (Å)	14.4237(9)
α(deg)	90
β(deg)	90
γ(deg)	90
V (Å^3)	7448.2(8)
Z	4
T (K)	180
F(000)	3056.0
D_{calc},g/cm^3	1.285
Total no. of data	13296
Crystal size (mm)	0.25×0.2×0.15
Completeness to θ	0.996
θ range	2.24-25.15
μ /mm^{-1}	0.115
Data/restraints/	13296/224
Parameters	1014
GoF on F^2	1.072
*R*1	0.0610

TMA_3PO_4 was added to a suspension of ligand (15 mg) in acetonitrile (3 mL), Then divide the mixture in to three parts after stirring overnight at room temperature in centrifugate. Then the mixture was centrifugate and filtered. The obtainer clear solution was used to crystals growing. Slow vapor of diethyl ether in to above-mentioner solution provided crystal of L•PO_4^{3-} (yellow) in one week. X-ray diffraction data were collected on a Bruker D8 Venture Photon II diffractometer at 180 K with graphite-monochromated Mo Kα radiation (λ = 0.71073 Å). An empirical absorption correction using SADABS was applied for all data (G. M. Sheldrick, Program SADABS: Area-Detector Absorption Correction, 1996, University of Göttingen, Germany). The structures were solved by the dual methods using the SHELXS program (G. Sheldrick, Acta Cryst. A, 2008, 64,

112-122). All non-hydrogen atoms were refined anisotropically by full-matrix least-squares on F2 using the program SHELXL, and hydrogen atoms were included in idealized positions with thermal parameters equivalent to 1.2 times those of the atom to which they were attached. It was noted that four countercations TMA^+ were confirmed, of which two TMA^+ cations (N atoms labelled as N19 and N20) have an occupancy of 0.5 thus making the total positive charges of +3. Therefore, the charges (negative and positive) of entire crystal structure are balanced. Four solvent molecules of CH_3CN were found in high disorder and all refined with partial occupancies (0.4-0.6). In addition, one CH_3CN (N22) molecule is found to partially overlap with one TMA^+ (N19) molecule.

The crystal data and refinement details are given in Table S1.

Table S2 Hydrogen bonding information in the crystal structure of $L^{NO2}\bullet PO_4^{3-}$.

D-H···*A*	d(*D*-H)	d(H···*A*)	d(D···*A*)	∠(*D*H*A*)
N2-H2···O13	0.88	2.00	2.806(7)	152
N3-H3···O14	0.88	2.10	2.886(7)	148
N4-H4···O14	0.88	1.90	2.760(6)	166
N5-H5···O15	0.88	1.89	2.741(5)	162
N7-H7···O13	0.88	2.00	2.762(6)	144
N8-H8···O15	0.88	2.05	2.869(6)	154
N9-H9···O15	0.88	1.86	2.733(6)	170
N10-H10···O16	0.88	2.01	2.800(8)	148
N12-H12···O13	0.88	2.03	2.780(6)	143
N13-H13···O16	0.88	2.00	2.860(6)	167
N14-H14···O16	0.88	1.89	2.760(6)	169
N15-H15···O14	0.88	1.91	2.778(6)	171
average	0.88	1.97±0.08	2.80±0.05	158±11

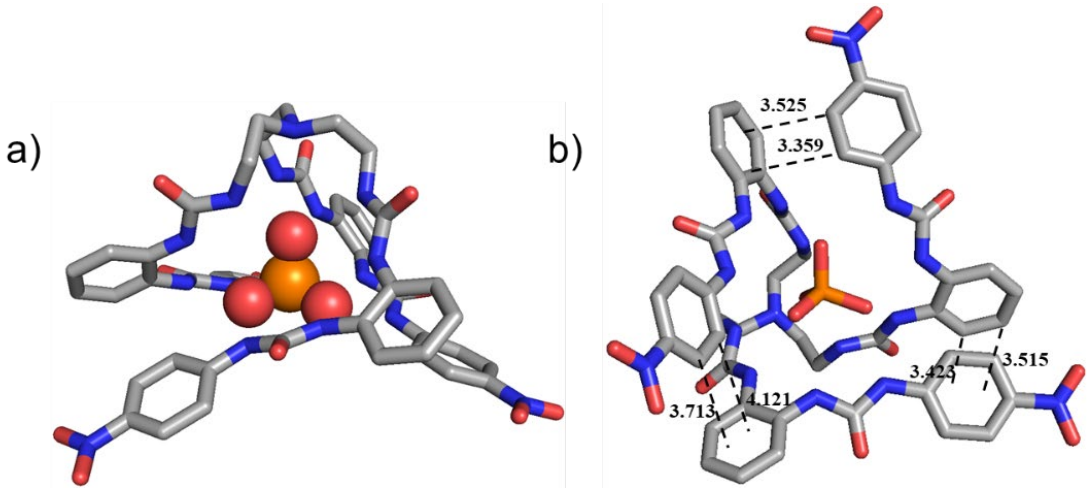

Figure S5 X-ray structure for the complex of PO_4^{3-} binding complex showing overall 1:1 stoichiometry. Secondary C-H···π within phenyl spacer and C−H atoms of terminal phenyl ring are shown on the right.

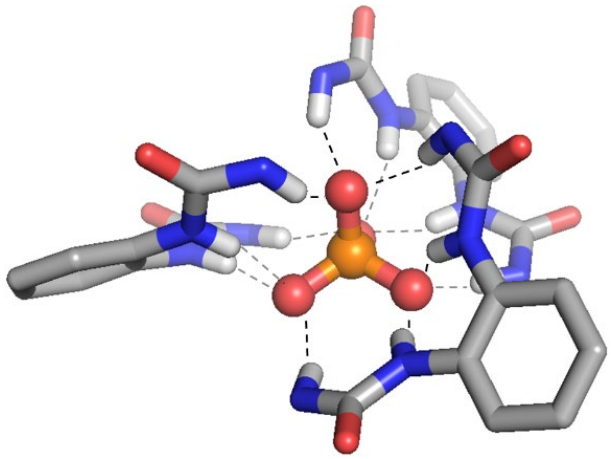

Figure S6 The hydrogen bonding networks seen in the PO_4^{3-} binding complex.

S4. Computational Studies for $H_2PO_4^-$ and HPO_4^{2-} Bindings

To get structural information for the complex upon binding to HPO_4^{2-} and $H_2PO_4^-$ anions, computational calculations were conducted by using Spartan' 20. We first tried a "bottom-up" approach by running "conformer distribution" with "molecular mechanics-MMFF" (energy barrier < 40 kJ/mol, at most 500 conformers). Unfortunately, given the highly flexible structure of hexaurea receptor, we were not able to complete this full calculation. Alternatively, we chose to calculate the structure based on rational designs by comparing to the crystal structure of PO_4^{3-} binding complex.

In the PO_4^{3-} binding complex, we see the lone pair of central N atom point towards the cavity which could potentially interact with HPO_4^{2-} and $H_2PO_4^-$ anions through O-H···N hydrogen bonding. Therefore, the conformer I was built based on this concept and optimized at the theory

level of ωB97X-D/6-31G(D). In contrast, the other conformer II was built as representative structure that did not include the O-H···N hydrogen bonding. The conformer was also optimized at the theory level of ωB97X-D/6-31G(D). Overall, we found that the conformer I was more energetically favored than the conformer II. According to the Boltzman population at 298 K, the conformer I was dominating with 100% for HPO_4^{2-} binding complex and about 65% for $H_2PO_4^-$ binding complex.

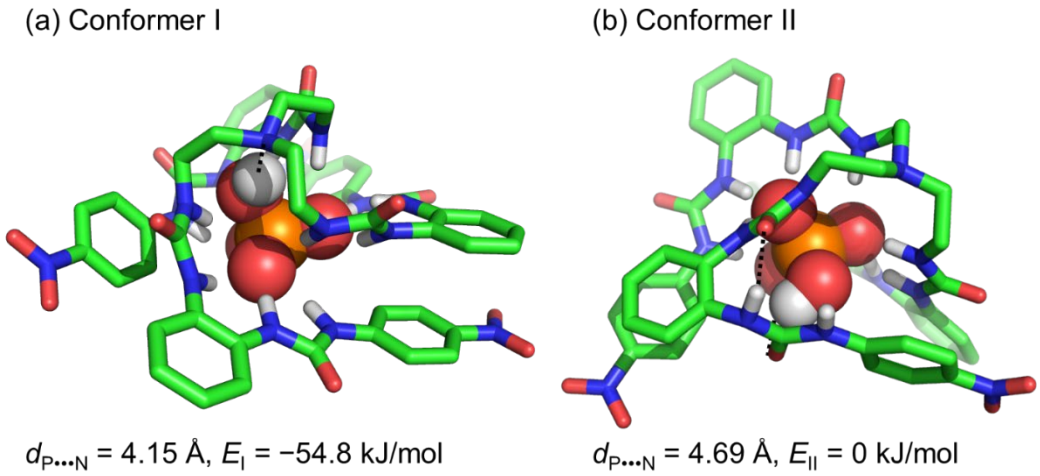

Figure S7 DFT-optimized structure of (a) conformer I and (b) conformer II for the HPO_4^{2-} binding complex by using Spartan 20 at the theory level of ωB97X-D/6-31G(D). In comparison, the conformer I is energetically favored by -54.8 kJ/mol. For conformer I, the OH of HPO_4^{2-} forms O-H···N hydrogen bonding with central N atom. For conformer II, the OH forms O-H···O=C hydrogen bonding with one of carbonyl groups.

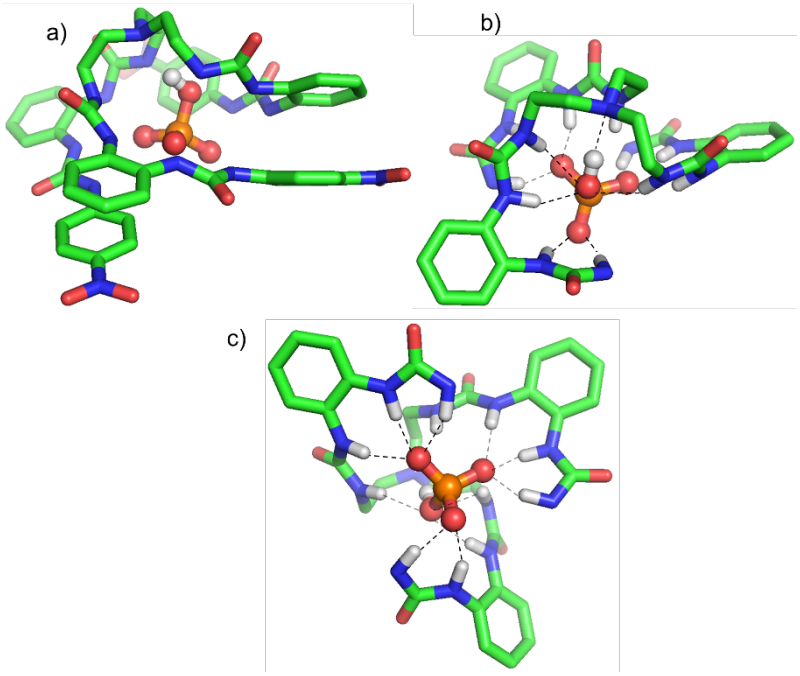

Figure S8 Hydrogen bonding networks seen in DFT-optimized structure of conformer I for the HPO_4^{2-} binding complex using Spartan 20 at the theory level of ωB97X-D/6-31G(D).

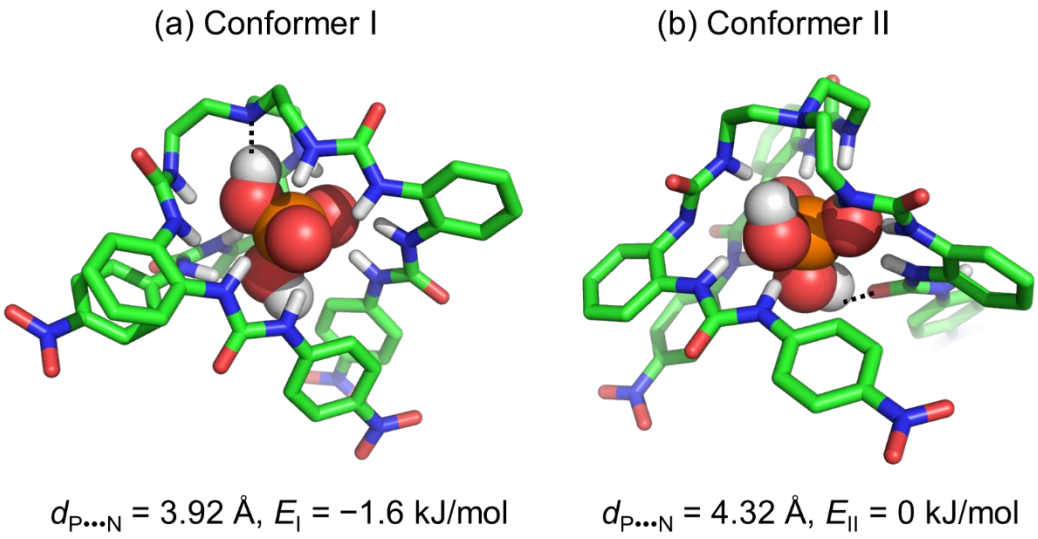

Figure S9 DFT-optimized structure of (a) conformer I and (b) conformer II for the $H_2PO_4^-$ binding complex by using Spartan 20 at the theory level of ωB97X-D/6-31G(D). In comparison, the conformer I is energetically favored. For the two conformers, only one of the two OH groups in $H_2PO_4^-$ can forms hydrogen bonds. specifically, for conformer I, one OH of $H_2PO_4^-$ forms O-H···N hydrogen bonding with central N atom. For conformer II, only one OH forms O-H···O=C hydrogen bonding with one of carbonyl groups.

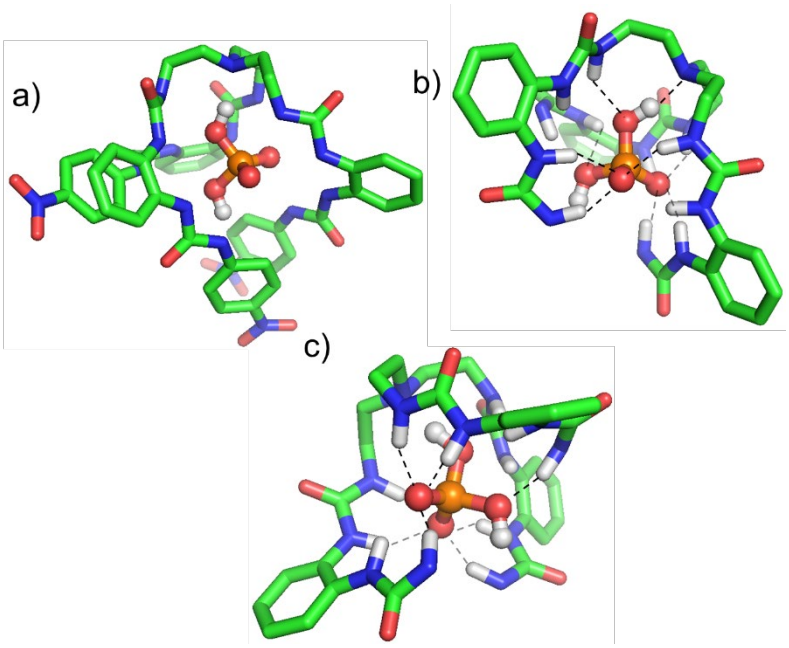

Figure S10 Hydrogen bonding networks seen in DFT-optimized structure of conformer I for the $H_2PO_4^-$ binding complex using Spartan 20 at the theory level of ωB97X-D/6-31G(D).

S5. ^{1}H NMR Studies for Anion Bindings

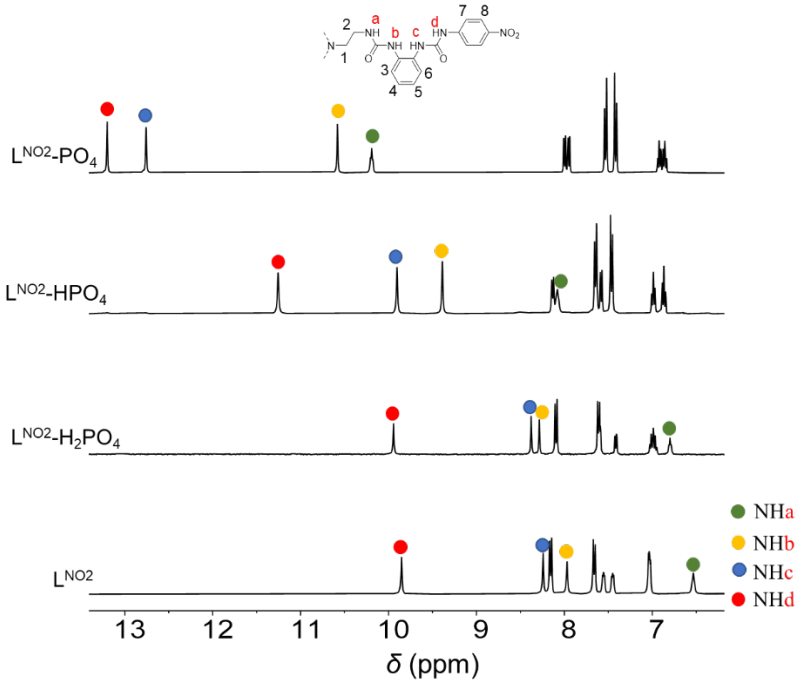

Figure S11 [1] Stacked partial ^{1}H NMR spectra (400 MHz, DMSO-d_6, 298 K, 2 mM) of the receptor

and its binding complex in the presence of one equivalent of different inorganic phosphate anions.

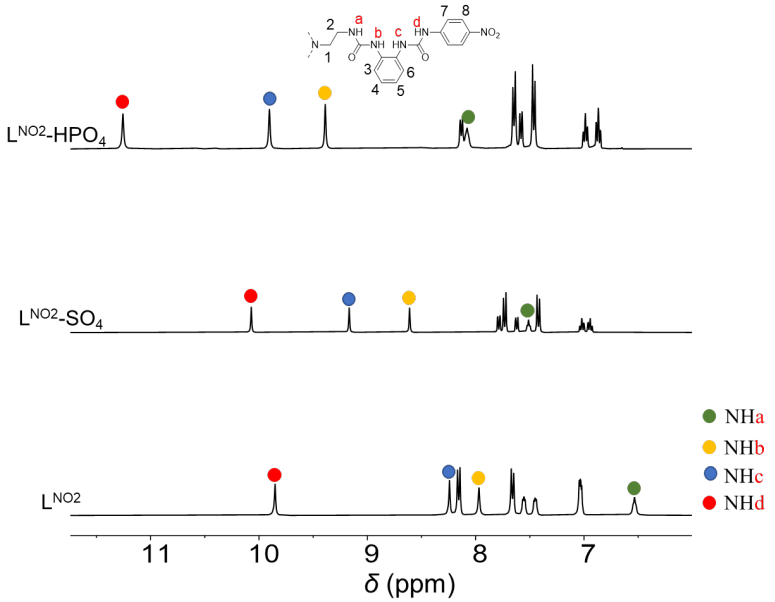

Figure S12 Stacked partial ^{1}H NMR spectra (400 MHz, DMSO-d_6, 298 K, 2 mM) of the receptor and the SO_4^{2-} and HPO_4^{2-} binding complexes. We observed that the chemical shifts of urea N-H in HPO_4^{2-} binding complex is relatively downfield shifted suggesting relatively strong HPO_4^{2-} binding than SO_4^{2-} binding.

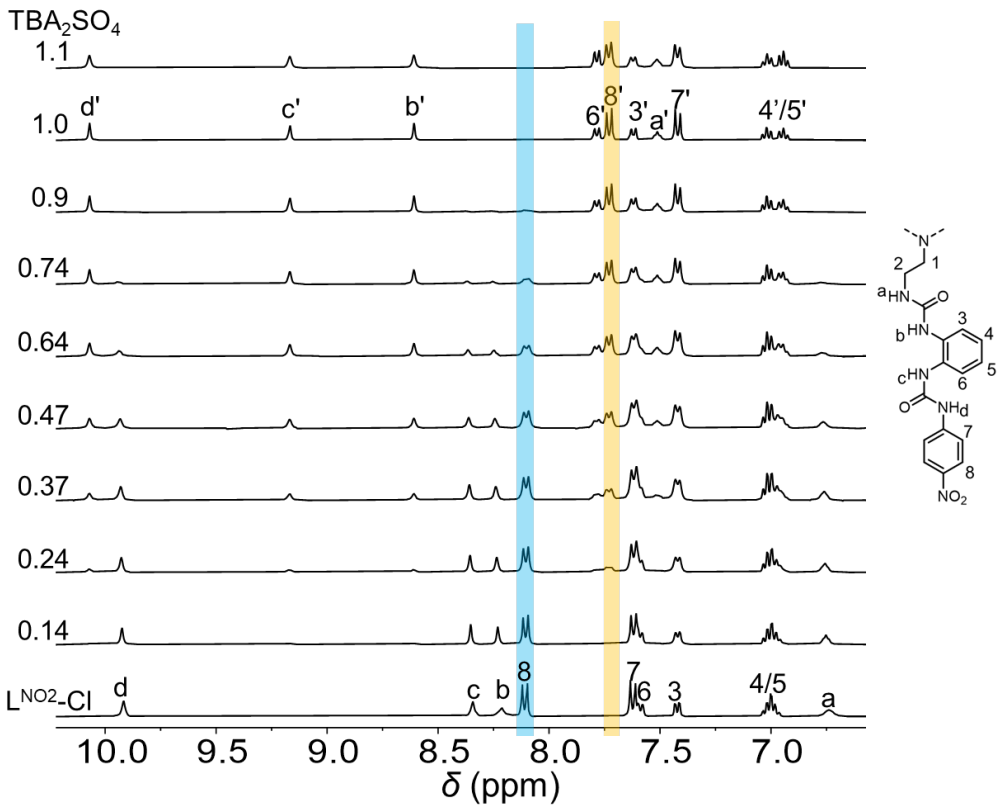

Figure S13 Stacked partial ^{1}H NMR spectra (400 MHz, 298 K, DMSO-d_6, 2 mM) of chloride binding complex by adding TBA_2SO_4 (50 mM).

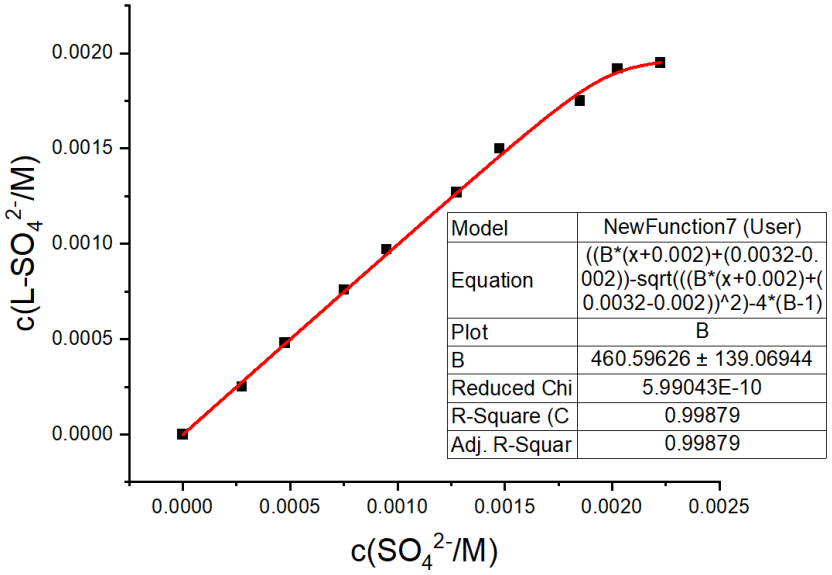

Figure S14 Fitted curve for the competitive titration between sulfate and chloride anions, which is derived from Figure S11. It indicates that sulfate binding affinity is 460-fold stronger than chloride.

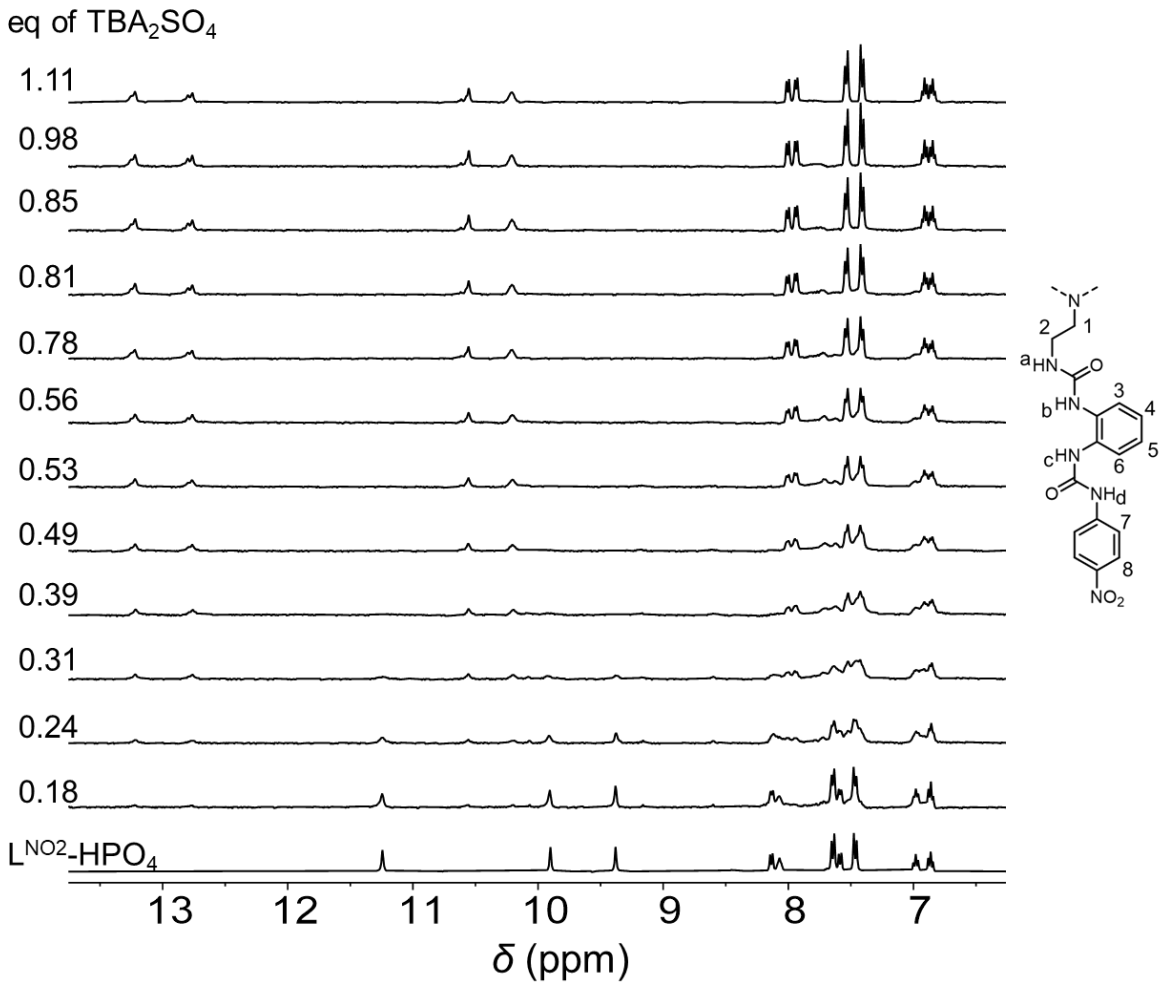

Figure S15 Stacked partial ^{1}H NMR spectra (400 MHz, 298 K, DMSO-d_6, 2 mM) of HPO_4^{2-} binding complex by TBA_2SO_4 (50 mM). Notably, addition of sulfate inducing the formation of PO_4^{3-} binding complex.

For the "hydrolysis" of PO_4^{3-}, it indicates the equilibrium: $PO_4^{3-} + H_2O \leftrightarrows HPO_4^{2-} + OH^-$. In regular DMSO solvent, the existence of water would facilitate such hydrolysis and produce HPO_4^{2-} anions, which interferes the titration. To minimize the interference, DMSO solvent was pre-dried over molecular sieves.

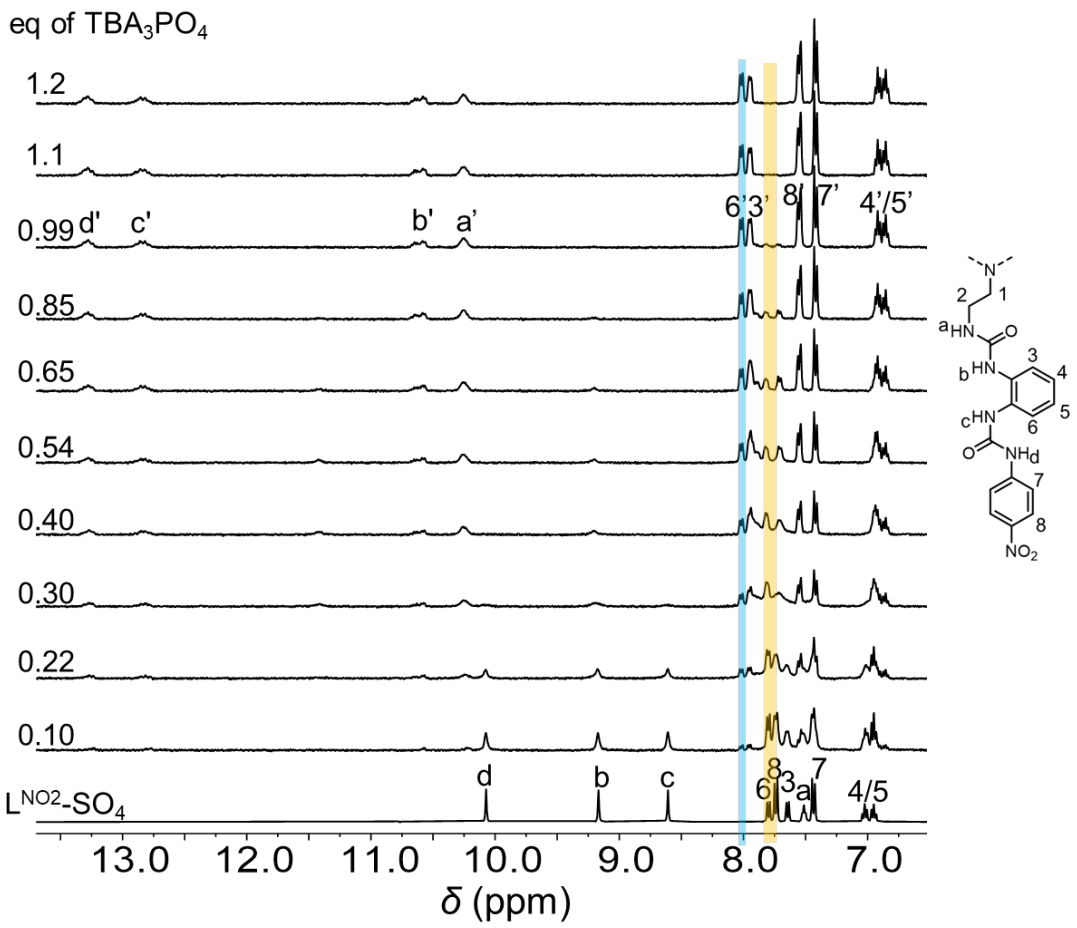

Figure S16 Stacked partial ^{1}H NMR spectra (400 MHz, 298 K, DMSO-d_6, 2 mM) of SO_4^{2-} binding complex by TBA_3PO_4 (50 mM).

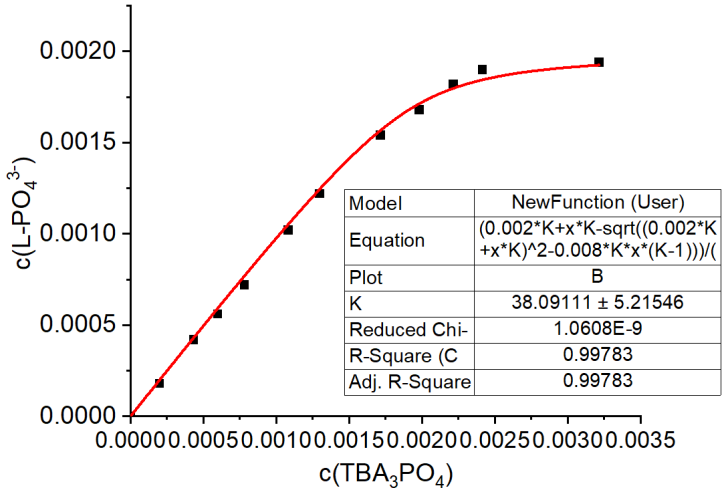

Figure S17 Fitted curve for the competitive titration between SO_4^{2-} binding and PO_4^{3-} binding, which is derived from Figure S14. It indicates that PO_4^{3-} binding affinity is 38-fold stronger than SO_4^{2-} binding.

S6. Liquid-Liquid Extraction Studies

S6.1 General liquid-liquid extraction procedure for ^{1}H NMR and IC analyses

Aqueous solutions (2 mL) containing the targeted anion salts (e.g., Na_3PO_4, Na_2HPO_4, NaH_2PO_4, 10 mM) were mixed with 2 mL of extractant L (10 mM) along with three equivalents of A336Cl in $CHCl_3$. Subsequent extraction involved vigorous shaking at room temperature for 20 seconds, leading to an immediate separation of the two solution phases. The aqueous layer (2 mL) was withdrawn and subjected to filtration through a 0.2 μM syringe filter before being analyzed on ion chromatography (IC). The organic layer (0.2 mL) was carefully collected, and the solvents were removed under reduced pressure and further dried on vacuum. The obtained sample was re-dissolved in DMSO-d_6 and subsequently subjected for ^{1}H NMR.

According to the literatures, p*K*a values of aryl ureas are typically large than 14 in DMSO (*J. Am. Chem. Soc.* **1991**, *113*, 8398; *Chem. Eur. J.* **2019**, *25*, 4695.) Therefore, the potential deprotonation of urea groups would be negligible. We tested the ^{1}H NMR spectra of organic layer after LLE with a basic aqueous solution (pH = 13.2) and found that the spectrum is comparable to the model spectra of PO_4^{3-} binding complex that was obtained from crystallization (Figure S18).

Table S3 Summery for the phosphate concentration that is remaining in water after extraction.

Ligand	Na_3PO_4		Na_2HPO_4		NaH_2PO_4	
	$c(H_xPO_4^{3-x})$	pH	$c(H_xPO_4^{3-x})$	pH	$c(H_xPO_4^{3-x})$	pH
L^{NO2}	1.96±0.05 79.9%	7.88	4.54±0.08 53%	6.3	8.53±0.06 15.5%	5.10

Note: The result was determined by IC. Only phosphate is present in water before extraction, and the initial concentration of phosphates is determined to be 9.72~9.81 mM.

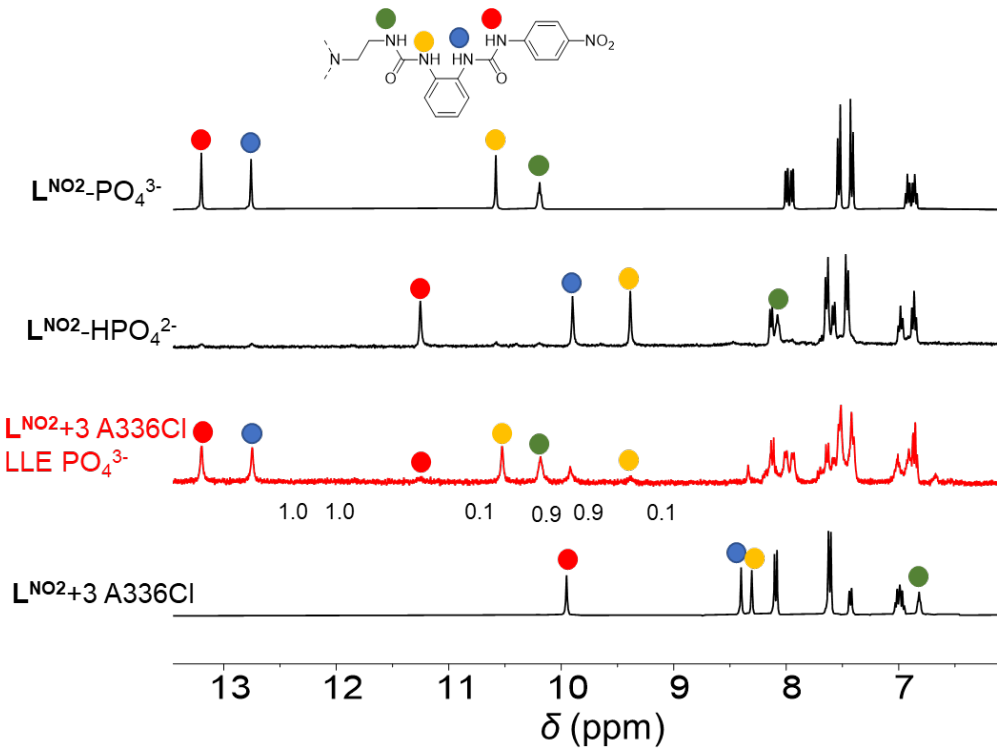

Figure S18 Stacked partial ^{1}H NMR (400 MHz, 298 K, DMSO-d_6), from bottom to top: **L** with three equivalents of A336Cl, the organic phase after LLE, model complexes for HPO_4^{2-} binding and PO_4^{3-} binding. This suggests that 82% of receptor was bound to phosphate after LLE.

Table S4 Remaining phosphate concentration and pH in water after extraction by increasing the amounts of receptors used for extraction.

Equivalents of receptors	**L**	
	c($H_xPO_4^{3-x}$)	pH
1.0	1.96±0.05 79.9%	7.88
1.2	1.55±0.01 84.1%	7.23
1.4	1.28±0.02 87.0%	7.10
1.6	1.15±0.05 88.5%	7.05
1.8	0.98±0.01 90%	6.88
2.0	0.97±0.02 90.1%	6.75

Table S5 Remaining monohydrogen phosphate concentration in water after extraction by increasing the amounts of receptors used for extraction.

Equivalents of receptors	L^{NO2} $c(H_xPO_4^{3-x})$	pH
1.0	4.54±0.08 55.5%	6.3
1.2	3.90±0.05 59.8%	6.07
1.4	3.75±0.05 61.3%	5.97
1.6	3.61±0.02 62.8%	5.86
1.8	3.57±0.06 63.2%	5.79

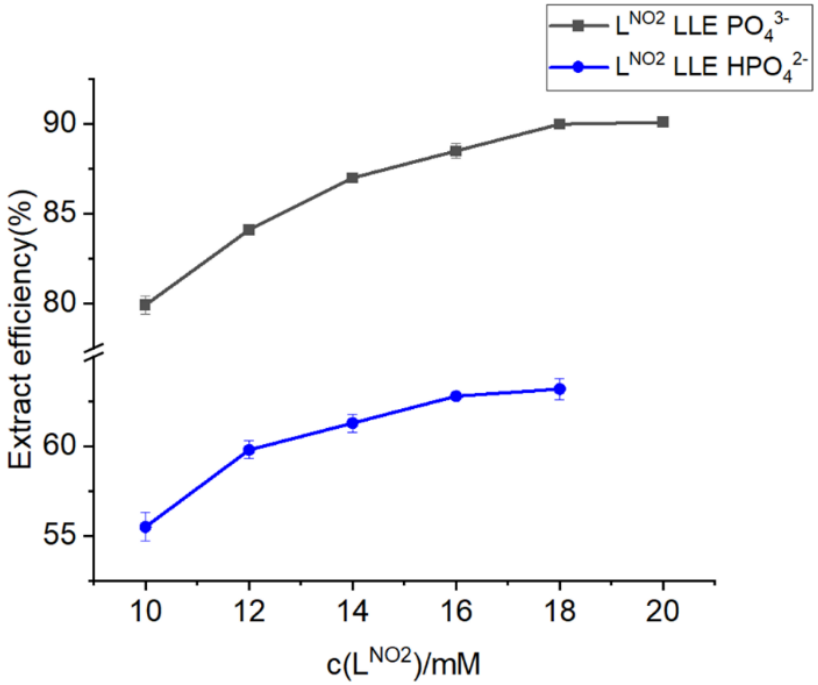

Figure S19 Extraction efficiency changes by increasing the amounts of receptors.

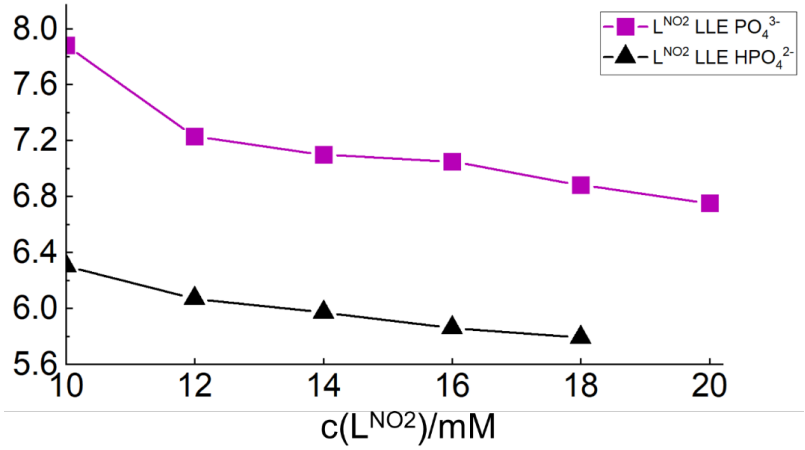

Figure S20 Changes of pH values after extraction by using different amounts of receptors for Na_3PO_4 and Na_2HPO_4 extraction.

Aqueous solutions (2 mL) containing Na_3PO_4 (0.1 mM, 1 mM, 2 mM, 10 mM) were subjected to exposure with one equivalent or two equivalents (2 mL) of receptor with three equivalents of A336Cl in $CHCl_3$. Subsequent extraction was achieved through vigorous shaking at room temperature for 20 seconds, resulting in immediate phase separation of the two solutions. The aqueous layer (2 mL) was extracted and passed through a 0.2 μM syringe filter before undergoing analysis using ion chromatography.

Table S6 Summery for the phosphate concentration that is remaining in water after extraction under different concentration.

eq of L^{NO2}	1eq		2eq	
	PO_4^{3-} remaining	pH	PO_4^{3-} remaining	pH
0.1 mM	0.06±0.01 44.7%	6.35	0.04±0.01 64.7%	6.45
1 mM	0.27±0.02 73.4%	7.30	0.09±0.01 91.3%	7.00
2 mM	0.37±0.03 80.2%	7.30	0.16±0.01 92.2%	7.03
5 mM	0.99±0.06 81.7%	7.45	0.33±0.02 93.2%	7.05
10 mM	1.7±0.07 83.4%	7.80	0.83±0.09 91.8%	6.80

Table S7 Summery for the phosphate concentration that is remaining in water after extraction under different concentration. The pH of phosphate source solution was adjusted to 12.

eq of L^{NO2}	1eq		2eq	
	PO_4^{3-} remaining	pH	PO_4^{3-} remaining	pH
0.1 mM	0.06±0.01 42.6%	12.06	0.03±0.01 70.0%	12.05
1 mM	0.44±0.07 56.4%	12.05	0.03±0.01 97.1%	12.00
2 mM	0.43±0.02 78.5%	11.99	0.04±0.01 98.1%	11.88
5 mM	1.09±0.08 78.3%	11.92	0.07±0.01 98.6%	11.71

Table *S8* Control liquid-liquid extraction experiment using A336Cl alone in organic layer.

EXP.	PO_4^{3-} before extraction (mM)	PO_4^{3-} after extraction (mM)
1		10.05
2	10.03	10.12
3		10.08

S6.2 Reversible phosphate uptake and release

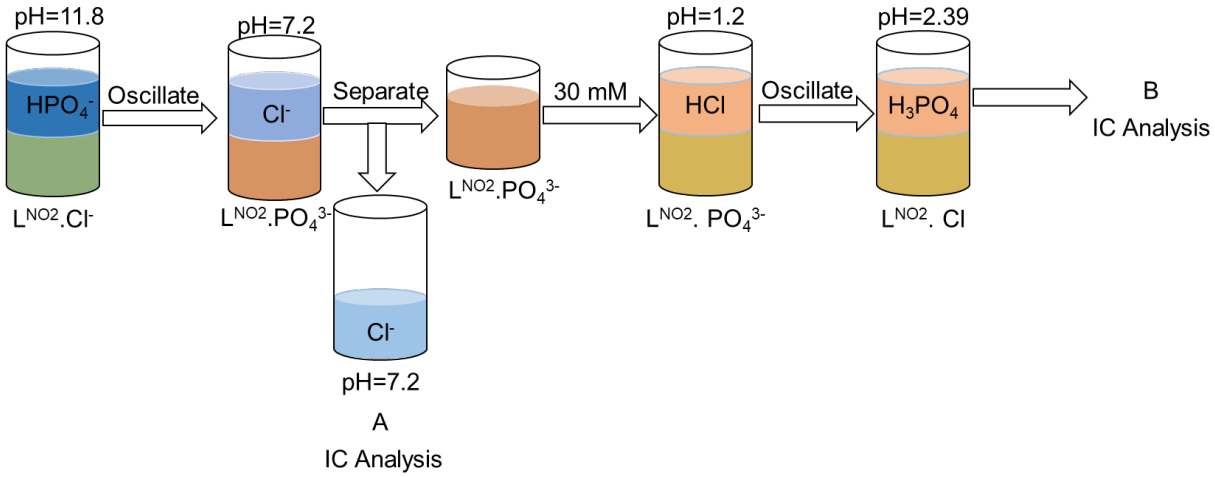

Figure S21 Diagram for the reversible phosphate uptake and release.

A centrifuge tube containing a solution of receptor (18 mM) along with three equivalents of A336Cl in $CHCl_3$ (2 mL) was combined with an aqueous solution of Na_3PO_4 (10 mM). The solutions were mixed by shaking for 20 seconds, and the resulting aqueous solution was carefully separated for subsequent IC analysis. The residual organic solution was then mixed with an aqueous solution of HCl (30 mM, 2 mL). After shaking for 20 seconds, the aqueous layer was separated for IC analysis. The remaining phosphate concentration in the aqueous phase was determined to be 1.06 mM, while the released phosphate concentration in the HCl solution was found to be 8.17 mM. The initial phosphate concentration was 10.07 mM.

S7 Separation of Phosphate and Sulfate Anions

S7.1 Stepwise extraction

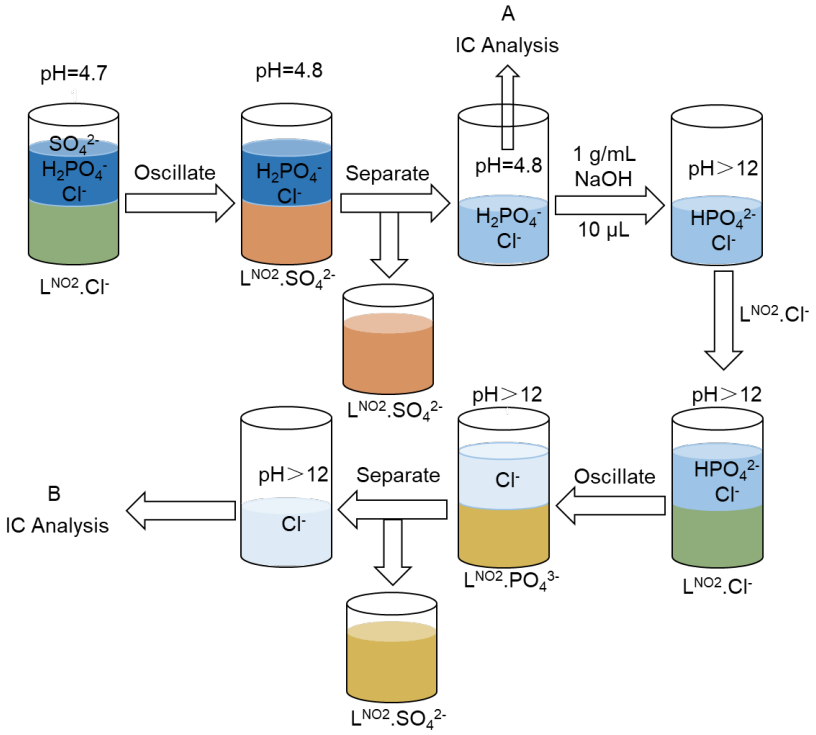

Figure S22 Diagram for the separation of phosphate and sulfate anions.

A solution comprising a mixture of anions, including $H_2PO_4^-$, Cl^-, and SO_4^{2-} (water phase, 10 mM), was subjected to treatment with a solution of receptor (13 mM) along with three equivalents of A336Cl in $CHCl_3$ (O1). Subsequently, the water phase and organic phase were separated. The water phase's pH was adjusted to 12 using a 25 M NaOH solution, followed by treatment of the water phase using a solution of receptor (20 mM) with three equivalents of A336Cl in $CHCl_3$ (O2). The water phase, after undergoing two successive extractions, was subjected to analysis through ion chromatography (IC).

Table S9 Concentration of various anions remaining and pH in water after extraction.

	PO_4^{3-}	SO_4^{2-}	Cl^-	pH
Before	10.2	10.0	10.1	4.7
A	9.5±0.1 93.3%	0.37±0.07 3.7%	30.5±0.2 304%	4.8
B	ND 0%	ND 0%	62±1 610%	＞12

S7.2 Post-extraction

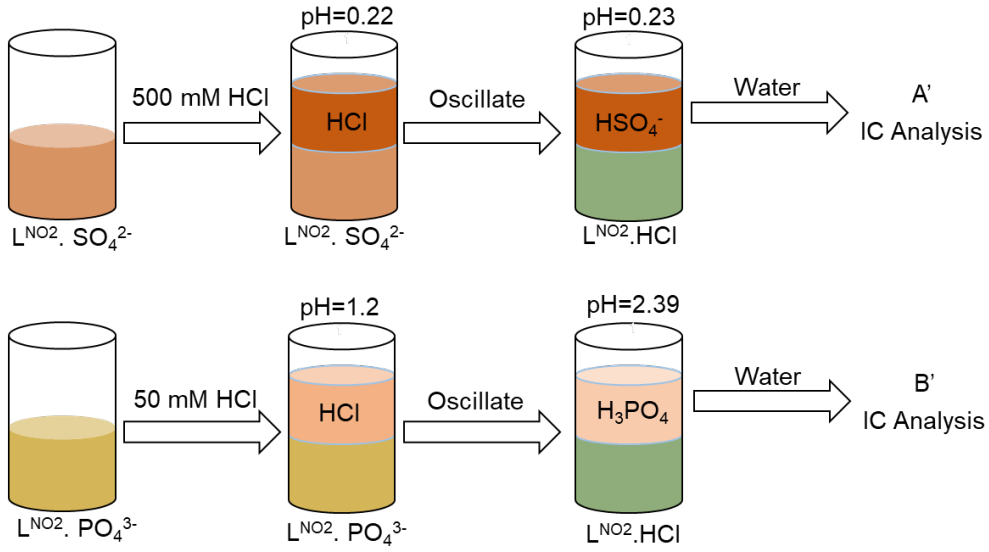

Figure S23 Diagram for the post-extraction. Regarding O1 (top), it was treated with 600 mM HCl, and the resulting HCl solution was analyzed using ion chromatography. In the case of O2 (bottom), it was treated with 50 mM HCl, and the HCl solution produced was also analyzed using ion chromatography.

Table S10 Concentration of PO_4^{3-}, $SO_4^{2-}$and pH in water after post-extraction with different concentration of HCl (50 mM/600 mM).

	PO_4^{3-}	SO_4^{2-}	pH
A'	ND 0%	9.0±0.2 90%	0.23
B'	9.3±0.1 93%	0.14±0.01 1.4%	2.39